ORIGINAL PAPER

CuO nanoparticles as a reusable catalyst for the synthesis of 1*H*-pyrazolo[1,2-*b*]phthalazine-5,10-dione derivatives under solvent-free conditions

Sonatai Patil[1] · Ananda Mane[2] · Savita Dhongade-Desai[1]

Abstract

Nanostructured CuO was successfully utilized for the synthesis of 1*H*-pyrazolo[1,2-*b*]phthalazine-5,10-dione derivatives via one-pot multicomponent reaction among phthalhydrazide, malononitrile and aromatic aldehydes under solvent-free conditions. Utilization of non-toxic and inexpensive catalyst, improved yields in short reaction times, wide substrate scope and easy purification of products are the important features of the developed protocol. The CuO nanocatalyst presents good reusability over five catalytic cycles.

Keywords CuO nanoparticles · 1*H*-Pyrazolo[1,2-*b*]phthalazine-5,10-diones · Solvent-free reaction · Heterogeneous catalyst · Multicomponent reaction · Nanocatalysis

Introduction

Nowadays, multicomponent reactions (MCRs) under solvent-free condition have emerged as a key green technology for the synthesis of medicinally relevant molecules from simple and readily available starting materials. Solvent-free organic synthesis allows the construction of various biologically active compounds by removing the harmful and flammable organic solvents which are a source of chemical contamination and produce large quantities of wastage. In most cases, the reactions performed under solvent-free condition are faster than conventional methods and produce high yield of products with low energy requirement. On the other hand, MCRs provide products in single step by designing number of bonds in one pot. MCRs offer significant advantages such as increased reaction rate, high atom economy, reduction of time and avoidance of complicated purification processes and tedious protection and deprotection of functional groups. These advantages make MCRs as an influential strategy for the synthesis of polyfunctionalized heterocyclic skeletons [1]. Among these, heterocycles containing fused 1*H*-pyrazolo[1,2-*b*]phthalazine-5,10-dione scaffold show intriguing biological activities [2–5] such as antimicrobial, antioxidant, antitubercular, analgesic, antipyretic, antihypoxant, antifungal and anti-acetylcholinesterase activities.

In view of the promising bioactivities, enormous synthetic methods have been developed for the synthesis of 1*H*-pyrazolo[1,2-*b*]phthalazine-5,10-dione derivatives. Among these, the most studied synthetic approach involves three-component condensation of an aromatic aldehyde, phthalhydrazide and malononitrile in presence of different catalytic systems such as triethylamine in ethanol under ultrasonication [6], mesoporous solid acid catalysts (Al-KIT-6) in ethanol at 60 °C [7], electrolysis in *n*-propanol [8], deep eutectic solvent [9], Bronsted solid acid catalyst containing double-charged diazoniabi-cyclo[2.2.2]octane chloride supported on rice husk silica nanoparticles (RH@[SiPrDABCO@BuSO$_3$H]HSO$_4$) [10], 1-butyl-3-methylimidazolium hydroxide [Bmim]OH under microwave irradiation [11], silicotungstic acid-coated amino-functionalized silica–magnetite nanoparticles in methanol under reflux condition [12] and *β*-cyclodextrin in water:ethanol solvent

✉ Sonatai Patil
  sonal_patil91@rediffmail.com

1 Research Laboratory in Heterocyclic Chemistry, Devchand College Arjunnagar, Kolhapur, M.S. 591269, India

2 Department of Chemistry, KIT's College of Engineering, Kolhapur, M.S. 416234, India

system at 100 °C [13]. In addition, the reactions under solvent-free condition involving different catalysts such as InCl$_3$ [14], *N,N,N′,N′*-tetrabromobenzene-1,3-disulfonamide (TBBDA) or poly(*N*-bromo-*N*-ethylbenzene-1,3-disulfonamide) (PBBS) [15], supported caesium carbonate [16], mesoporous silica nanocomposite [17], metal oxide nanoparticles [18, 19] and ionic liquids [20–22] also led to formation of 1*H*-pyrazolo[1,2-*b*]phthalazine-5,10-diones. Nevertheless, most of the existing methodologies have one or more drawbacks such as the use of hazardous organic solvents, expensive and large amounts of catalyst requirement, prolonged reaction time and lack of reusability of the catalyst. Therefore, the development of new methodologies which could overcome these drawbacks is highly desirable.

It has been established that nanoparticles could be used successfully as catalysts for organic transformations to get highly selective products. Nanocatalysts offer practical advantages such as easy separation form reaction mixture, high potential for selectivity, high thermal stability, good structural stability and large number of active sites on the surface. In this context, copper oxide nanoparticles (CuO NPs) have gained substantial attention from synthetic organic chemists due to their unique physical and chemical properties namely high surface area, non-flammability, inexpensiveness, operational simplicity and reusability [23]. CuO NPs mediated carbon–carbon and carbon–heteroatom bond formation reactions have evolved as useful methods for the synthesis of heterocyclic compounds [24–27]. Moreover, CuO NPs endorsed solvent-free reactions have also been reported in organic transformations for the synthesis of bioactive molecules [28–32]. In addition, CuO nanostructures have been extensively investigated by researchers because of their promising applications in various fields such as electrochemical cells [33], gas sensors [34], bio-sensors [35], photovoltaic cells [36], thermoelectric materials [23], nanofluids [37], photocatalysis [38] and removal of inorganic pollutants [39].

Taking all these facts into account herein, we disclosed a facile one-pot synthesis of 1*H*-pyrazolo[1,2-*b*]phthalazine-5,10-diones via three-component reaction of various aromatic aldehydes, phthalhydrazide and malononitrile in the presence of catalytic amount of CuO NPs under solvent-free condition at 100 °C with good to excellent yields.

Experimental

All the chemicals were obtained from Merck Company and used as received. The melting points of products were measured in open capillary tubes. Infrared spectra were recorded on Perkin Elmer FT-IR spectrometer. ^{1}H and ^{13}C NMR spectra were recorded on a Bruker-Avance 300 MHz spectrometer using TMS as an internal standard and DMSO-d_6 as a

solvent. Mass spectra were recorded on Shimadzu QP 2010 GCMS. The X-ray diffraction (XRD) measurements of the catalyst powder were recorded by a Phillips diffractometer of X'pert company with monochromatized Cu Kα radiation ($\lambda = 1.5406$ Å). Microscopic morphology of nanocatalyst was visualized by field emission scanning electron microscopy (FESEM) (LEO 1455VP).

Preparation of CuO nanoparticles

In a flask, 9.0 g of copper(II) chloride dihydrate was dissolved in minimum amount of ethanol. Then in a separate flask 5.4 g of sodium hydroxide pellets were dissolved in minimum amount of ethanol as required. The prepared sodium hydroxide solution was then added dropwise to copper(II) chloride dihydrate solution with constant stirring at room temperature. During addition, the colour of solution turned from green to bluish green and finally to black as the reaction proceeded. The obtained black precipitate of copper hydroxide was filtered by centrifuge, washed with ethanol and deionized water and then dried at about 50 °C in the dryer. The dried sample was annealed into a muffle furnace at 400 °C for 5 h to obtain crystalline CuO NPs.

General procedure for synthesis 1*H*-pyrazolo[1,2-*b*] phthalazine-5,10-diones

A mixture of phthalhydrazide (1 mmol), malononitrile (1 mmol), aldehyde (1 mmol) and CuO NPs (10 mol%) was stirred at 100 °C under solvent-free condition for required time. The progress of the reaction was monitored by thin-layer chromatography (TLC, petroleum ether:ethyl acetate, 8:2). After completion, the reaction mixture was cooled and residue obtained was solved in 10 mL of ethyl acetate and centrifuged to separate the CuO NPs. Evaporation of solvent left the crude solid product which was recrystallized from ethanol to afford the pure 1*H*-pyrazolo[1,2-*b*]phthalazine-5,10-dione derivatives.

3-Amino-5,10-dioxo-1-phenyl-5,10-1*H*-pyrazolo[1,2-b] phthalazine-2-carbonitrile (4a) Pale yellow solid; mp 274–276 °C. FT-IR (KBr, cm^{-1}): 3362, 2198, 1660, 1601. ^{1}H NMR (300 MHz, DMSO-d_6, δ ppm): 6.21 (s, 1H, CH), 7.40–7.53 (m, 5H, Ar–H), 8.03 (bs, 2H, NH$_2$), 8.18 (t, $J = 5.7$ Hz, 3H, Ar–H), 8.36 (dd, $J = 3.6$ Hz, $J = 6.0$ Hz, 1H, Ar–H). ^{13}C NMR (75 MHz, DMSO-d_6, δ ppm): 61.8, 63.5, 100.0, 116.3, 127.1, 127.2, 127.7, 128.7, 128.9, 129.0, 129.1, 134.1, 135.0, 138.6, 151.0, 154.0, 157.0.

3-Amino-1-(4-chlorophenyl)-5,10-dihydro-5,10-dioxo-1*H*-pyrazolo[1,2-b]phthalazine-2-carbonitrile (4b) Pale yellow solid; mp 266–268 °C. FT-IR (KBr, cm^{-1}): 3363, 3261, 2196, 1660. ^{1}H NMR (300 MHz, DMSO-d_6, δ ppm):

6.16 (s, 1H, CH), 7.44 (d, $J = 8.4$ Hz, 2H, Ar–H), 7.54 (d, $J = 8.4$ Hz, 2H, Ar–H), 7.97 (bs, 2H, NH_2), 8.09–8.14 (m, 3H, Ar–H), 8.26–8.29 (m, 1H, Ar–H). ^{13}C NMR (75 MHz, DMSO-d_6, δ ppm): 61.6, 62.8, 100.0, 116.9, 126.9, 128.2, 129.5, 133.5, 135.2, 138.0, 151.3, 154.4, 157.4.

3-Amino-5,10-dihydro-5,10-dioxo-1-p-tolyl-1H-pyrazolo[1, 2-b]phthalazine-2-carbonitrile (4f) Yellow solid; mp 255–257 °C. FT-IR (KBr, cm^{-1}): 3362, 3258, 2196, 1654, 1560. ^{1}H NMR (300 MHz, DMSO-d_6, δ ppm): 2.30 (s, 3H, CH_3), 6.06 (s, 1H, CH), 7.14 (d, $J = 7.5$ Hz, 2H, Ar–H), 7.29 (d, $J = 7.8$ Hz, 2H, Ar–H), 7.90 (t, 2H, NH_2), 8.04–8.10 (m, 3H, Ar–H), 8.25 (dd, $J = 3.0$ Hz, $J = 5.7$ Hz, 1H, Ar–H). ^{13}C NMR (75 MHz, DMSO-d_6, δ ppm): 21.2, 61.7, 63.3, 116.1, 127.1, 127.2, 127.7, 128.9, 129.0, 129.4, 133.8, 134.8, 135.2, 138.1, 150.9, 153.8, 156.8.

3-Amino-1-(4-cyanophenyl)-5,10-dihydro-5,10-dioxo-1H-pyrazolo[1,2-b]phthalazine-2-carbonitrile (4g) Yellow solid; mp 230–232 °C. FT-IR (KBr, cm^{-1}): 3420, 3315, 2204, 1664, 1557. ^{1}H NMR (300 MHz, DMSO-d_6, δ ppm): 6.18 (s, 1H, CH), 7.63 (d, $J = 8.1$ Hz, 2H, Ar–H), 7.73 (d, $J = 7.2$ Hz, 2H, Ar–H), 7.90 (t, 2H, NH_2), 8.07–8.11 (m, 3H, Ar–H), 8.27 (dd, $J = 3.6$ Hz, $J = 6.6$ Hz, 1H, Ar–H). ^{13}C NMR (75 MHz, DMSO-d_6, δ ppm): 60.9, 62.8, 111.4, 116.2, 127.1, 127.7, 128.1, 128.9, 129.4, 133.0, 134.3, 135.1, 144.4, 151.3, 154.2, 157.1.

3-Amino-1-(2-chlorophenyl)-5,10-dihydro-5,10-dioxo-1H-pyrazolo[1,2-b]phthalazine-2-carbonitrile (4h) Pale yellow solid; mp 268–270 °C. FT-IR (KBr, cm^{-1}): 3373, 3176, 2210, 1679, 1659. ^{1}H NMR (300 MHz, DMSO-d_6, δ ppm): 6.44 (s, 1H, CH), 7.28 (bs, 2H, NH_2), 7.37 (t, 2H, Ar–H), 7.89 (d, $J = 4.2$ Hz, 2H, Ar–H) 8.05–8.10 (m, 3H, Ar–H), 8.27 (t, 1H, Ar–H). ^{13}C NMR (75 MHz, DMSO-d_6, δ ppm): 60.2, 61.4, 115.7, 127.2, 127.8, 127.9, 128.5, 128.8, 130.1, 130.2, 132.0, 134.1, 135.0, 151.5, 153.8, 156.9.

3-Amino-1-(3-nitrophenyl)-5,10-dihydro-5,10-dioxo-1H-pyrazolo[1,2-b]phthalazine-2-carbonitrile (4 k) Pale yellow solid; mp 269–271 °C. FT-IR (KBr, cm^{-1}): 3433, 3323, 2198, 1658, 1602. ^{1}H NMR (300 MHz, DMSO-d_6, δ ppm): 6.33 (s, 1H, CH), 7.66 (d, $J = 7.8$ Hz, 1H, Ar–H), 7.94 (bs, 2H, NH_2), 8.08–8.38 (m, 7H, Ar–H). ^{13}C NMR (75 MHz, DMSO-d_6, δ ppm): 60.6, 62.7, 100.0, 116.1, 122.5, 123.7, 127.7, 128.9, 129.3, 130.4, 134.12, 134.17, 134.9, 140.8, 148.4, 151.5, 154.3, 157.1.

3-Amino-5,10-dioxo-1-(pyridin-4-yl)-5,10-dihydro-1H-pyrazolo[1,2-b]phthalazine-2-carbonitrile (4n) Pale yellow solid; mp 230–232 °C. FT-IR (KBr, cm^{-1}): 3368, 3265, 2193, 1654. ^{1}H NMR (300 MHz, DMSO-d_6, δ ppm): 6.17 (s, 1H, CH), 7.32 (dd, $J = 4.8$ Hz, $J = 7.8$ Hz, 1H,

Ar–H), 7.78 (bs, 2H, NH_2), 7.81–7.93 (m, 1H, Ar–H), 8.09 (t, $J = 3.3$ Hz, 3H, Ar–H), 8.24–8.27 (m, 1H, Ar–H), 8.48 (s, 1H, Ar–H), 8.65 (s, 1H, Ar–H). ^{13}C NMR (75 MHz, DMSO-d_6, δ ppm): 60.3, 61.4, 116.0, 123.9, 127.2, 127.8, 128.9, 133.5, 134.0, 134.9, 135.1, 149.0, 149.9, 151.4.

Results and discussion

FT-IR spectrum (Fig. 1) of synthesized CuO NPs shows two absorption bands at 519 cm^{-1} and 473 cm^{-1}, assigned to the Cu(II)–O stretching vibrations in CuO. A broad absorption band at 3600–3200 cm^{-1} and a band at 1633 cm^{-1} correspond to O–H stretching and H–O–H bending vibrations of water adsorbed on nanostructured CuO surface and water absorbed by KBr.

The powder XRD pattern (Fig. 2) of synthesized CuO NPs was indexed to the monoclinic structure with lattice constants of $a = 4.6476$ Å, $b = 3.4259$ Å and $c = 5.0539$ Å and $\beta = 99.3890°$. The diffraction peaks at $2\theta = 32.48°$, 35.50°, 38.72°, 48.77°, 53.45°, 58.23°, 61.59°, 66.32°, 68.02°, 72.42° and 75.13° correspond to the phases such as (110), (002/−111), (111/200), (−202), (020), (202), (−113), (022/−311), (220/113), (311) and (004/−222), respectively (JCPDS: 72-0629) [40]. The average crystalline size of CuO NPs was found to be 16 nm, determined from full-width at half-maxima (FWHM) at reflection (111) plane using Debye Scherrer formula.

The EDS analysis (Fig. 3) confirms the presence of copper and oxygen as the only elementary components in synthesized CuO NPs. In addition, a small carbon peak was also observed due to the used carbon tape. The FESEM images (Fig. 4) revealed the surface morphology of CuO NPs as well-dispersed nanosphere architecture with grain size approximately 66 nm.

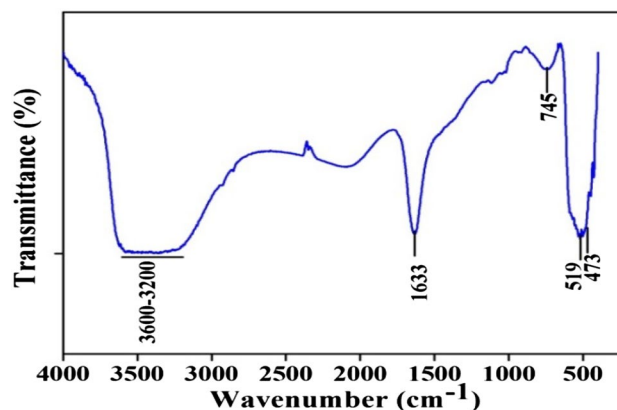Our initial investigation for optimization of reaction parameters focused on the reaction of phthalhydrazide (**1**),

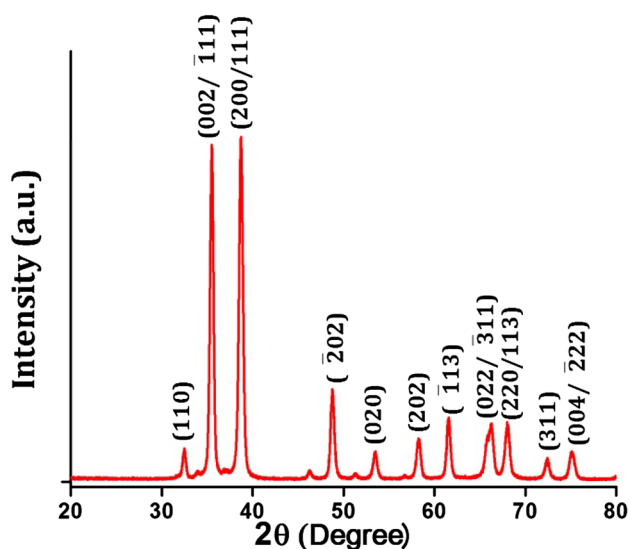**Fig. 1** FT-IR spectrum of CuO NPs

Fig. 2 Powder X-ray diffraction pattern of CuO NPs

malononitrile (**2**) and benzaldehyde (**3a**) as model reaction (Scheme 1).

When the model reaction was run in water with 10 mol% of CuO NPs at room temperature, no formation of desired product **4a** was noticed even after stirring for 180 min (Table 1, entry 1). After screening different organic solvents such as ethanol, acetonitrile, toluene for model reaction, trace amount of product formation was noted (Table 1, entries 2–4). Therefore, to increase the product yield, the model reaction was run in different solvents at refluxing temperatures as different reaction behaviours may originate from differences in solvent and reaction temperature. It observed that the reaction was effective in protic solvents such as ethanol, *n*-propanol, acetonitrile, 1,2-dichloroethane and

improved reaction rates and product yields were achieved (Table 1, entries 5–8); whereas in aprotic solvents such as tetrahydrofuran, toluene and *n*-hexane the reaction was very slow and resulted in lower yield of product (Table 1, entries 9–11). Furthermore, the model reaction was conducted under solvent-free condition at 80 °C in presence of 10 mol% of CuO NPs and 84% yield of product **4a** was noted within 30 min (Table 1, entry 12). In our endeavour to enhance the yield of **4a,** the model reaction was investigated at 100 °C and surprisingly 94% product yield was noted within 20 min (Table 1, entry 13). It was also observed that further increase in reaction temperature to 120 °C had no positive effect on product yield (Table 1, entry 14). To substantiate the role of catalyst, the model reaction was carried out at 100 °C in the absence of catalyst under solvent-free condition and trace amount of product formation was noted (Table 1, entry 15). In most of the solvents, the reaction rate was slower and desired product was obtained in moderate yield, whereas solvent-free condition provided superior yield in short reaction time. The better yield in solvent-free condition could be due to the closer proximity of reactants to react than in reaction conditions using different solvents. Subsequently, we have screened the different amount of CuO NPs for model reaction at 100 °C and results are summarized in Table 2 (entries 1–6). When 6, 8, 9, 10, 11 and 12 mol% of CuO NPs were used the yields were 72%, 80%, 86%, 94%, 94% and 94%, respectively. Therefore, it confirmed that 10 mol% of CuO NPs was sufficient and increase in amount of catalyst further to 12 mol% did not improve the yield significantly. On the basis of above-mentioned observations, we have concluded that 10 mol% of CuO NPs at 100 °C under neat condition was the optimum reaction condition for the synthesis of fused 1*H*-pyrazolo[1,2-*b*]phthalazine-5,10-diones.
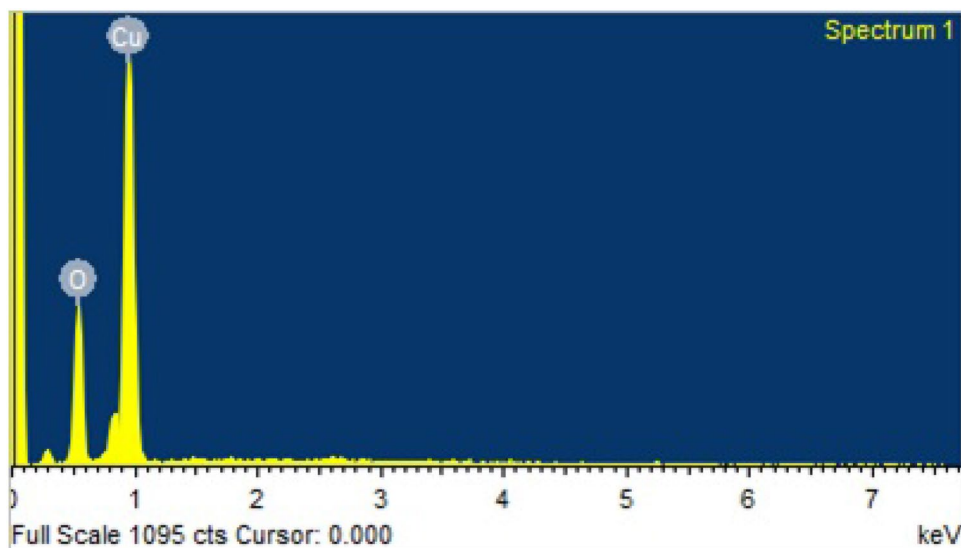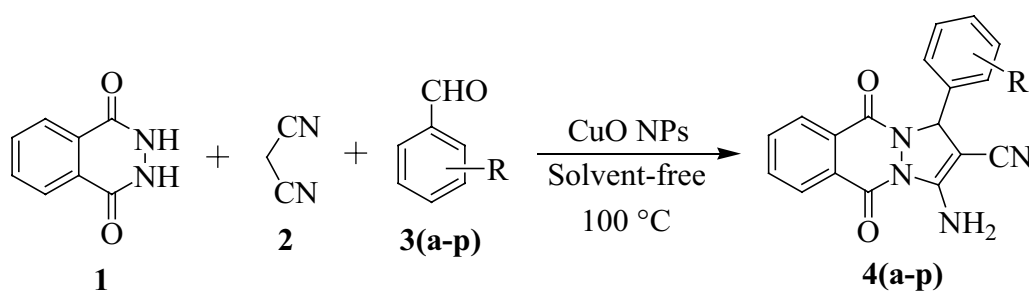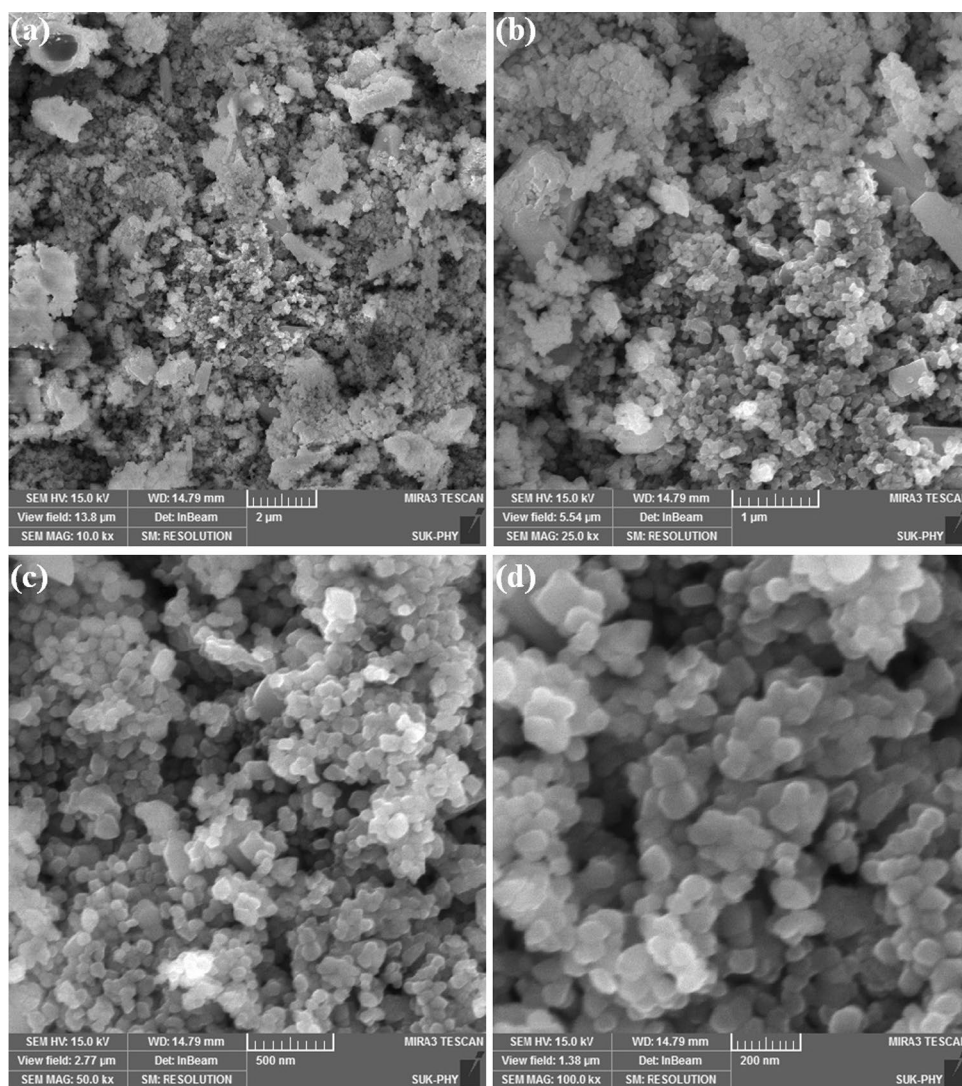
Fig. 3 EDS spectrum of CuO NPs

Fig. 4 SEM images of CuO NPs (**a**–**d**): low to high magnified view

Scheme 1 Solvent-free synthesis of 1H-pyrazolo[1,2-*b*]phthalazine-5,10-diones catalysed by CuO NPs

Next, in order to explore the efficiency of proposed protocol to a library system, various aldehydes **3(a–p)** were subjected to react with phthalhydrazide and malononitrile to yield corresponding 1*H*-pyrazolo[1,2-*b*]phthalazine-5,10-diones **4(a–p)** as shown in Table 3 (entries 1–16). It observed that the optimized reaction conditions are mild enough to tolerate various functional groups present on aromatic ring of aldehydes. It was noteworthy that,

Table 1 Influence of solvent and temperature on the yield of model reaction

Entry	Solvent	Temperature (°C)	Reaction time[a] (min)	Yield[b] (%)
1	Water	Room temperature	180	No reaction
2	Ethanol	Room temperature	180	Trace
3	Acetonitrile	Room temperature	180	Trace
4	Toluene	Room temperature	180	Trace
5	Ethanol	78	120	78
6	n-Propanol	97	120	80
7	Acetonitrile	82	120	74
8	1,2-Dichloroethane	83	120	82
9	Tetrahydrofuran	66	120	42
10	Toluene	111	120	35
11	n-Hexane	68	120	45
12	Solvent-free	80	30	84
13	Solvent-free	100	20	94
14	Solvent-free	120	20	92
15	Solvent-free	100	20	Trace[c]

Reaction conditions: phthalhydrazide (1 mmol), malononitrile (1 mmol), aldehyde (1 mmol) and CuO NPs (10 mol%) under stirring condition at different reaction temperatures

[a]Reaction progress monitored by TLC

[b]Isolated yield after purification

[c]Reaction was performed without catalyst

Table 2 Influence of amount of catalyst on the yield of model reaction

Entry	Amount of catalyst (mol%)	Reaction time[a] (min)	Yield[b] (%)
1	6	20	72
2	8	20	80
3	9	20	86
4	10	20	94
5	11	20	94
6	12	20	94

Reaction conditions: phthalhydrazide (1 mmol), malononitrile (1 mmol), aldehyde (1 mmol) and CuO NPs under solvent-free condition at 100 °C

[a]Reaction progress monitored by TLC

[b]Isolated yield after purification

the electronic nature of substituents on aromatic ring of aldehydes had no critical effect on product yield and aldehydes bearing electron-withdrawing or electron-donating substituents undergoes smooth reaction to furnish desired pyrazolo derivatives with good to excellent yields. However, it observed that increasing the steric hindrance close to the reaction centre reactivity of aldehyde was depressed, which causes yield decrement (entries 2–10). The reactions of aldehydes with electron-donating groups (–OCH$_3$, –CH$_3$) had a slightly higher reaction rate than the reactions of aldehydes with electron-withdrawing groups (–Cl, –F, –NO$_2$, –CN). Similarly, other substituted aldehydes (entries 11–13) reacted to deliver the desired products in moderate to good yields. It is important to note that the heteroaromatic aldehydes such as 4-pyridinecarboxaldehyde, pyrrole-2-carboxaldehyde and 2-thiophenecarboxaldehyde also reacted with equal ease to afford the desired products in excellent yields (entries 14–16).

Next, we have investigated the reusability of CuO NPs for the synthesis of 1*H*-pyrazolo[1,2-*b*]phthalazine-5,10-dione (**4a**, Scheme 1, Table 3). After the completion of reaction as indicated by TLC, the nanocatalyst was separated by centrifugation using ethyl acetate as solvent. The recovered catalyst was washed thoroughly with water (2×2 mL) and ethyl acetate (2×2 mL) to remove all adsorbed organic substrates from its surface and then dried in an oven at 100 °C. After that the dried catalyst was subjected to fresh reactants in model reaction to afford **4a** in 92% yield. The same procedure was repeated four more times and results obtained as shown in Fig. 5 indicates that CuO NPs could be reused up to five times without significant loss of catalytic activity.

In order to reveal the merits of present methodology, the catalytic efficiency of prepared CuO NPs for the synthesis of 1*H*-pyrazolo[1,2-*b*]phthalazine-5,10-dione (**4a**, Scheme 1, Table 3) has been compared with some of the previously reported catalysts. From the comparison as shown in Table 4, it is evident that the developed methodology is superior to most of the reported procedures in terms of reaction time and percentage yield.

In view of the above-mentioned results, a possible reaction mechanism for the formation of 1*H*-pyrazolo[1,2-*b*] phthalazine-5,10-dione (**4a**) is depicted in Fig. 6. Initially, the activation of C-H bond in malononitrile (**2**) by basic oxygen in the catalyst leads to the attack of malononitrile on activated carbonyl group of aldehyde (**3a**) under the catalytic effect of Lewis acidic sites of CuO NPs. The generated Knoevenagel adduct (**A**) undergoes Michael-type addition reaction with phthalhydrazide (**1**) to form iminomethylene intermediate (**B**) which on subsequent intramolecular cyclization and tautomerization in presence of CuO NPs gives the desired product **4a**.

Table 3 CuO NPs catalysed synthesis of 1*H*-pyrazolo[1,2-*b*]phthalazine-5,10-diones under solvent-free conditions
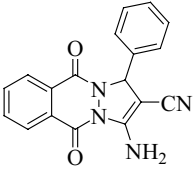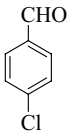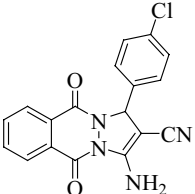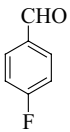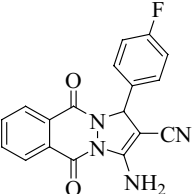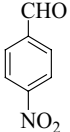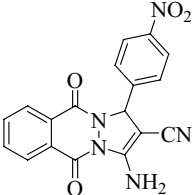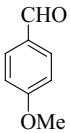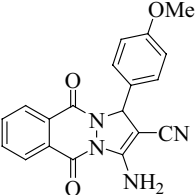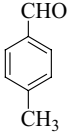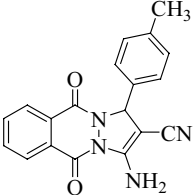
Entry	Aldehyde	Reaction time[a] (min)	Product	Yield[b] (%)	Mp (°C) [References]
1	CHO **3a**	20	**4a**	94	274–276 [12]
2	CHO / Cl **3b**	18	**4b**	94	266–268 [12]
3	CHO / F **3c**	18	**4c**	92	262–264 [6]
4	CHO / NO₂ **3d**	15	**4d**	94	260–262 [12]
5	CHO / OMe **3e**	30	**4e**	90	240–242 [12]
6	CHO / CH₃ **3f**	25	**4f**	89	255–257 [16]

Table 3 (continued)
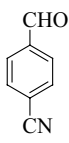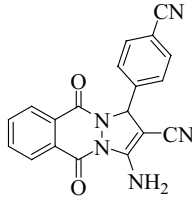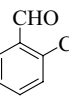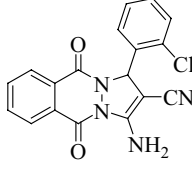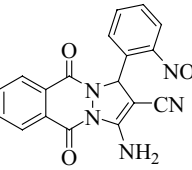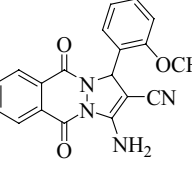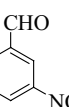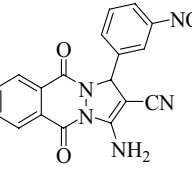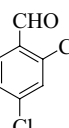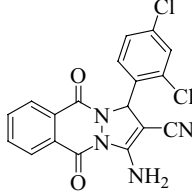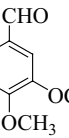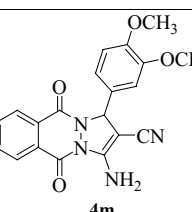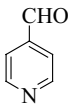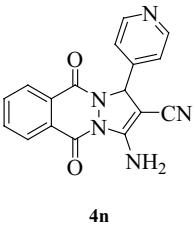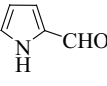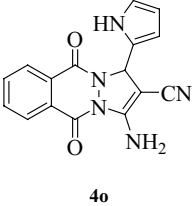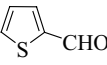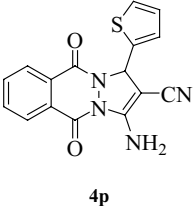
7	3g	20	4g	91	230–232 [13]
8	3h	25	4h	88	268–270 [16]
9	3i	20	4i	89	260–262 [17]
10	3j	30	4j	86	154–156 [16]
11	3k	20	4k	91	269–271 [12]
12	3l	20	4l	88	230–232 [18]
13	3m	30	4m	86	233–236 [12]

Table 3 (continued)

14	**3n**	25	**4n**	86	230–232 [16]
15	**3o**	35	**4o**	90	260–262 [12]
16	**3p**	35	**4p**	88	244–246 [16]

Reaction conditions: phthalhydrazide (1 mmol), malononitrile (1 mmol), aldehyde (1 mmol) and CuO NPs (10 mol%) under solvent-free condition at 100 °C

[a]Reaction progress monitored by TLC

[b]Isolated yield after purification
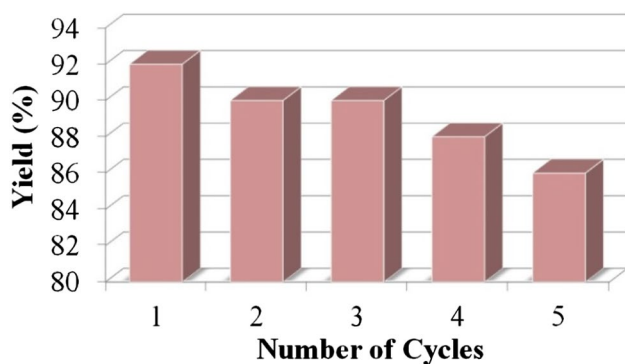
Fig. 5 Recyclability of CuO NPs for the synthesis of 1H-pyrazolo[1,2-b]phthalazine-5,10-dione (**4a**)

Conclusions

In summary, we have developed a sustainable method for the synthesis of 1H-pyrazolo[1,2-b]phthalazine-5,10-dione derivatives in one-pot reaction using CuO NPs under solvent-free conditions. The reactions are remarkably tolerant towards various functional groups present on aromatic ring of aldehydes and no side product or decomposition product was observed. In terms of green chemistry, the present method has several advantages such as recyclability of catalyst, higher isolated yields, shorter reaction times and avoidance of polluting and hazardous solvents.

Table 4 Comparison of the catalytic efficiency of CuO NPs with some reported catalysts for the synthesis of product **4a**

Entry	Catalyst	Catalyst amount	Reaction conditions	Time (min)	Yield (%)	References
1	Et$_3$N	20 mol%	Ethanol, 50 °C, ultrasonic irradiation	60	92	[6]
2	Al-KIT-6	300 mg	Ethanol, 60 °C	240	93	[7]
3	RH@[SiPrDABCO@BuSO$_3$H]HSO$_4$	0.15 gm	Ethanol, reflux	180	89	[10]
4	[Bmim]OH	0.2 mL	Microwave irradiation, 45 °C	4	94	[11]
5	STA–amine–Si–magnetite	10 mg	Methanol, 60 °C	45	98	[12]
6	β-Cyclodextrin	20 mol%	Water: ethanol (4:1), 100 °C	150	86	[13]
7	ZnO NPs	15 mol%	Solvent-free, 100 °C	14	90	[18]
8	(a) TBBDA	0.05 gm	Solvent-free, 100 °C	15	89	[15]
	(b) PBBS	0.05 gm	Solvent-free, 100 °C	40	65	
9	*p*-Toluenesulphonic acid	0.3 mmol	[bmim]Br, 100 °C	180	94	[20]
10	Supported caesium carbonate (Ni$_{0.5}$Zn$_{0.5}$Fe$_2$O$_4$@HAP–Cs$_2$CO$_3$)	0.02 gm	Solvent-free, 110 °C	15	93	[16]
11	Dicationic 4,4′-bipyridine silica hybrid nanocomposite, SBA@BiPy^{2+} 2Cl$^-$	0.005 gm	Solvent-free, 100 °C	40	96	[17]
12	1-(Copperferritesiloxypropyl)-3-methyl-imidazolium heteropolytungstate ionic liquid BW$_{12}$-ILMNPs	0.05 gm	Solvent-free, 80 °C	10	90	[21]
13	CuO NPs	10 mol%	Solvent-free, 100 °C	20	94	This work
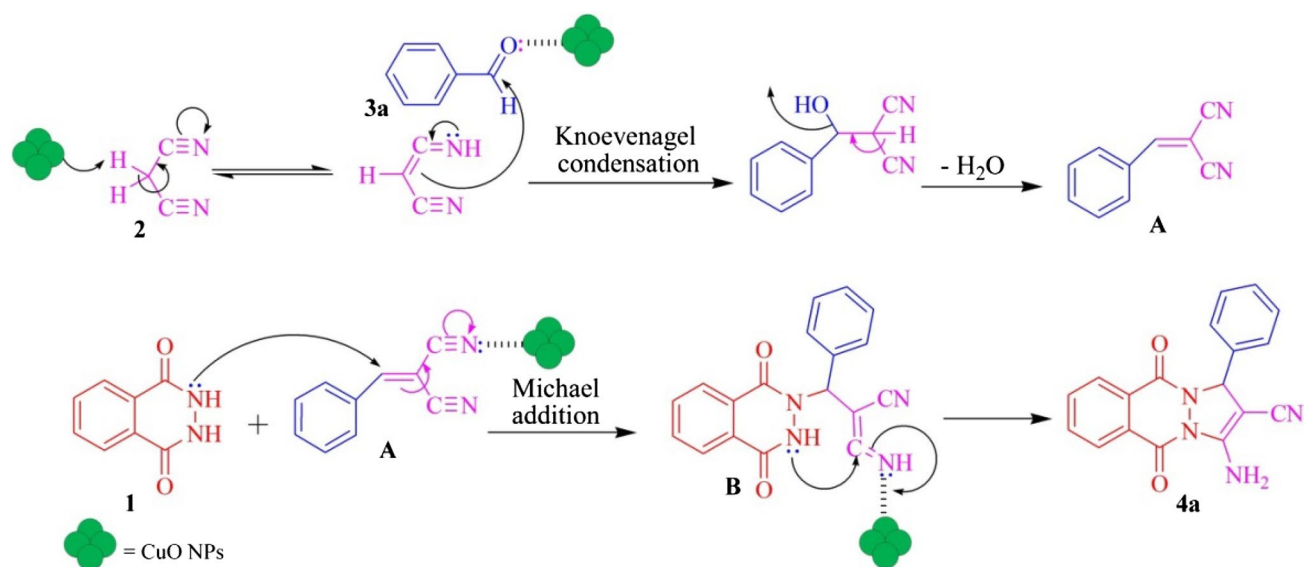
Fig. 6 Proposed mechanism for reaction between phthalhydrazide **1**, malononitrile **2** and benzaldehyde **3a** for generation of 1*H*-pyrazolo[1,2-*b*] phthalazine-5,10-dione **4a**

References

1. I.A. Ibarra, A. Islas-Jacome, E. Gonzalez-Zamora, Org. Biomol. Chem. **16**, 1402 (2018)
2. C.B. Sangani, J.A. Makwana, Y.-T. Duan, N.J. Thumar, M.-Y. Zhao, Y.S. Patel, H.-L. Zhu, Res. Chem. Intermed. **42**, 2101 (2016)

3. F. Al'-Assar, K.N. Zelenin, E.E. Lesiovskaya, I.P. Bezhan, B.A. Chakchir, Pharm. Chem. J. **36**, 598 (2002)
4. P.S.V. Kumar, L. Suresh, G.V.P. Chandramouli, J. Saudi Chem. Soc. **21**, 306 (2017)
5. L. Jalili-Baleh, H. Nadri, A. Moradi, S.N. Abbas Burkhari, M. Shakibaie, M. Jafari, M. Golshani, F.H. Moghadam, L. Firoozpour, A. Asadipour, S. Emami, M. Khoobi, A. Foroumadi, Eur. J. Med. Chem. **139**, 280 (2017)
6. M.R. Nabid, S.J.T. Rezaei, R. Ghahremanzadeh, A. Bazgir, Ultrason. Sonochem. **17**, 159 (2010)
7. G. Karthikeyan, A. Pandurangan, J. Mol. Catal. A Chem. **58**, 361–362 (2012)
8. H. Kefayati, S.H. Amlashi, R. Kazemi-Rad, A. Delafrooz, C. R. Chim. **17**, 894 (2014)
9. A. Chaskar, Curr. Catal. **3**, 266 (2014)
10. J. Davarpanah, A.R. Kiasat, RSC Adv. **5**, 7986 (2015)
11. D.S. Raghuvanshi, K.N. Singh, Tetrahedron Lett. **52**, 5702 (2011)
12. P. Arora, J.K. Rajput, Appl. Organomet. Chem. **32**, e4001 (2018)
13. Y.A. Tayade, D.S. Dalal, Catal. Lett. **147**, 1411 (2017)
14. M.V. Reddy, Y.T. Jeong, Tetrahedron Lett. **54**, 3546 (2013)
15. R. Ghorbani-Vaghei, S. Noori, Z. Toghraei-Semiromi, Z. Salimi, RSC Adv. **4**, 47925 (2014)
16. B. Maleki, S.B.N. Chalaki, S.S. Ashrafi, E.R. Seresht, F. Moeinpour, A. Khojastehnezhad, R. Tayebee, Appl. Organomet. Chem. **29**, 290 (2015)
17. A. Bashti, A.R. Kiasat, B. Mokhtari, RSC Adv. **5**, 25816 (2015)
18. A. Azarifar, R. Nejat-Yami, D. Azarifar, J. Iran. Chem. Soc. **10**, 297 (2013)
19. R. Tayebee, B. Maleki, M. Sabeti, J. Iran. Chem. Soc. **14**, 1179 (2017)
20. R. Ghahremanzadeh, G.I. Shakibaei, A. Bazgir, Synlett **8**, 1129 (2008)
21. H.R. Saadati-Moshtaghin, F.M. Zonoz, J. Nanostruct. Chem. **7**, 317 (2017)
22. F.H. Sabour, M. Nasr-Esfahani, I. Mohammadpoor-Baltork, S. Tangestaninejad, M. Moghadam, V. Mirkhani, J. Iran. Chem. Soc. **15**, 671 (2018)
23. Q. Zhang, K. Zhang, D. Xu, G. Yang, H. Huang, F. Nie, C. Liu, S. Yang, Prog. Mater Sci. **60**, 208 (2014)
24. S.J. Ahmadi, S. Sadjadi, M. Hosseinpour, M. Outokesh, R. Hekmatshoar, Catal. Commun. **10**, 1423 (2009)
25. S. Payra, A. Saha, S. Guchhait, S. Banerjee, RSC Adv. **6**, 33462 (2016)
26. M. Nasrollahzadeh, S.M. Sajadi, A. Rostami-Vartooni, S.M. Hussin, J. Colloid Interface Sci. **466**, 113 (2016)
27. P.K. Raul, A. Mahanta, U. Bora, A.J. Thakur, V. Veer, Tetrahedron Lett. **56**, 7069 (2015)
28. G.R. Chaudhary, P. Bansal, N. Kaur, S.K. Mehta, RSC Adv. **4**, 49462 (2014)
29. A. Fazlinia, S. Sheikh, Inorg. Nano Met. Chem. **48**, 126 (2018)
30. M.V. Reddy, Y.T. Jeong, RSC Adv. **6**, 103838 (2016)
31. G. Purohit, U.C. Rajesh, D.S. Rawat, ACS Sustain. Chem. Eng. **5**, 6466 (2017)
32. M. Rawat, D.S. Rawat, Tetrahedron Lett. **59**, 2341 (2018)
33. M. Kong, W. Zhang, Z. Yang, S. Weng, Z. Chen, Appl. Surf. Sci. **258**, 1317 (2011)
34. C. Yang, X. Su, J. Wang, X. Cao, S. Wang, L. Zhang, Sens. Actuators B Chem. **185**, 159 (2013)
35. Md.M. Rahman, A.J.S. Ahammad, J.-H. Jin, S.J. Ahn, J.-J. Lee, Sensors **10**, 4855 (2010)
36. C.C. Vidyasagar, Y.A. Naik, T.G. Venkatesh, R. Viswanatha, Powder Technol. **214**, 337 (2011)
37. L.-P. Zhou, B.-X. Wang, X.-F. Peng, X.-Z. Du, Y.-P. Yang, Adv. Mech. Eng. (2010) https://doi.org/10.1155/2010/172085
38. M.M. Sarafraz, F. Hormozi, Exp. Therm. Fluid Sci. **52**, 205 (2014)
39. I. Ali, Chem. Rev. **112**, 5073 (2012)
40. D. Han, H. Yang, C. Zhu, F. Wang, Powder Technol. **185**, 286 (2008)